2001-10-29
43rd APS DPP BP1-056
Long Beach, USA

Full wave analysis of ICRF waves and Alfvén eigenmodes in toroidal plasmas

A. Fukuyama and T. Akutsu
Department of Nuclear Engineering,
Kyoto University, Kyoto 606-8501, Japan

Supported by Grant-in-Aid for Scientific Research of the Ministry of Education, Culture, Sports, Science and Technology, Japan and the collaboration programme of the National Institute for Fusion Science.

Abstract

In order to investigate the behavior of ICRF waves and Alfvén eigenmodes in toroidal plasmas, such as tokamaks and toroidal helical devices, we have revised the full wave code TASK/WM to deal with the plasma with three-dimensional inhomogeneity. We solved Maxwell's equation as a boundary-value problem in the flux coordinates and the response of the plasma is described by a dielectric tensor including kinetic effects. First we analyze propagation and absorption of the ICRF waves in LHD plasmas. Next we analyze the Alfvén eigenmodes both within and below the toroidicity-induced frequency gap in tokamaks. The effects of toroidal plasma rotation and reversed magnetic shear are studied. Mode-structure of RTAE and excitation by energetic ions are also studied.

Linear Stability Analysis of Alfvén Eigenmode

- **MHD Analysis** (Ideal, Resistive)
- **MHD including Kinetic Effect** (perturbative)
  - Eigen function from MHD analysis, Growth rate including kinetic effects
- **Kinetic Analysis** (Electron thermal motion, Ion gyromotion, Drift motion)
  - PENN code (Jaun, Alfvén Lab)
  - TASK/WM (Fukuyama)
- **Ballooning Expansion** (High n mode)
  - HINST (Gorelenkov, Cheng)
  - 2D-WKB (Vlad, Chen, Zonka)
- **3D Full Wave Code: TASK/WM**
  - Magnetic surface coordinates from MHD Equilibrium Analysis
  - Boundary value problem of Maxwell's equation. Dielectric tensor)
  - Fourier mode expansion in poloidal and toroidal direction, FDM in radius)
  - Looking for complex eigen frequency which maximize the integral of wave field.

Full Wave Code: TASK/WM

- **Magnetic Flux Coordinates** **(Non-Orthogonal)**
  - Minor radius direction: Poloidal Magnetic Flux ψ
  - Poloidal direction: θ
  - Toroidal direction: φ

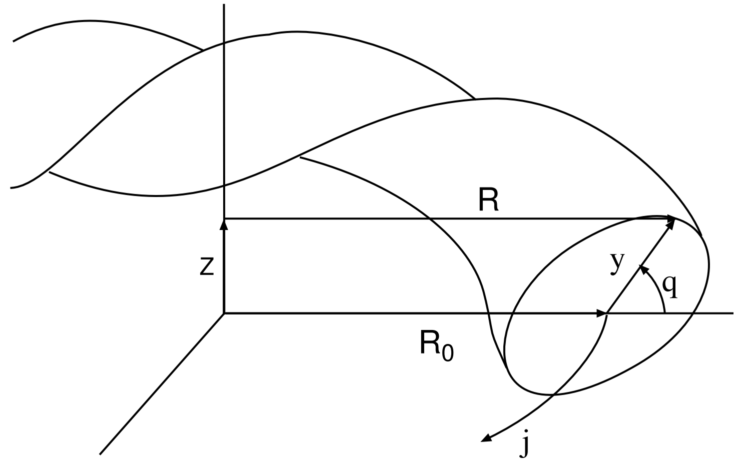

- **Co-variant expression** of $\boldsymbol{E}$

$$\boldsymbol{E} = E_1\boldsymbol{e}^1 + E_2\boldsymbol{e}^2 + E_3\boldsymbol{e}^3$$

where contra-variant basis

$$\boldsymbol{e}^1 = \boldsymbol{\nabla}\psi, \qquad \boldsymbol{e}^2 = \boldsymbol{\nabla}\theta, \qquad \boldsymbol{e}^3 = \boldsymbol{\nabla}\varphi$$

- J **: Jacobian** $\quad J = \dfrac{1}{\boldsymbol{e}^1 \cdot \boldsymbol{e}^2 \times \boldsymbol{e}^3} = \dfrac{1}{\boldsymbol{\nabla}\psi \cdot \boldsymbol{\nabla}\theta \times \boldsymbol{\nabla}\varphi}$

- g **: Metric tensor** $\quad g_{ij} = \boldsymbol{e}_i \cdot \boldsymbol{e}_j$, where co-variant basis $\boldsymbol{e}_i \equiv \partial\boldsymbol{r}/\partial x_i$

Wave Equation

- **Maxwell's equation** for stationary wave electric field $\boldsymbol{E}$

  (angular frequency ω, light velocity c)

$$\nabla \times \nabla \times \boldsymbol{E} = \frac{\omega^2}{c^2} \overleftrightarrow{\epsilon} \cdot \boldsymbol{E} + \mathrm{i}\,\omega \mu_0 \boldsymbol{j}_{\mathrm{ext}}$$

  - $\overleftrightarrow{\epsilon}$: **Dielectric Tensor** : Effects of finite temperature

    Cyclotron damping, Landau damping

  - $\boldsymbol{j}_{\mathrm{ext}}$: Antenna Current

- **Wave Equation in Non-Orthogonal Coordinates** (radial components)

$$(\nabla \times \nabla \times \boldsymbol{E})^1 = \frac{1}{J}\left[\frac{\partial}{\partial x^2}\left\{\frac{g_{31}}{J}\left(\frac{\partial E_3}{\partial x^2} - \frac{\partial E_2}{\partial x^3}\right) + \frac{g_{32}}{J}\left(\frac{\partial E_1}{\partial x^3} - \frac{\partial E_3}{\partial x^1}\right) + \frac{g_{33}}{J}\left(\frac{\partial E_2}{\partial x^1} - \frac{\partial E_1}{\partial x^2}\right)\right\}\right.$$
$$\left. - \frac{\partial}{\partial x^3}\left\{\frac{g_{21}}{J}\left(\frac{\partial E_3}{\partial x^2} - \frac{\partial E_2}{\partial x^3}\right) + \frac{g_{22}}{J}\left(\frac{\partial E_1}{\partial x^3} - \frac{\partial E_3}{\partial x^1}\right) + \frac{g_{23}}{J}\left(\frac{\partial E_2}{\partial x^1} - \frac{\partial E_1}{\partial x^2}\right)\right\}\right]$$

  - $(x^1, x^2, x^3) = (\psi, \theta, \varphi)$
  - Similar expression for poloidal and toroidal components

Response of Plasmas

- Usually the dielectric tensor $\overleftrightarrow{\epsilon}$ is calculated in Cartesian coordinates with static magnetic field along the z axis.
- **Local normalized orthogonal coordinates**

$$\hat{\boldsymbol{e}}_s = \frac{\boldsymbol{\nabla}\psi}{|\boldsymbol{\nabla}\psi|}, \quad \hat{\boldsymbol{e}}_b = \hat{\boldsymbol{e}}_h \times \hat{\boldsymbol{e}}_\psi, \quad \hat{\boldsymbol{e}}_h = \frac{\boldsymbol{B}_0}{|\boldsymbol{B}_0|}$$

- Variable Transformation: $\overleftrightarrow{\mu}$

$$\begin{pmatrix} E_1 \\ E_2 \\ E_3 \end{pmatrix} = \overleftrightarrow{\mu} \cdot \begin{pmatrix} E_s \\ E_b \\ E_h \end{pmatrix}$$

$$\overleftrightarrow{\mu} \equiv \begin{pmatrix} \dfrac{1}{\sqrt{g^{11}}} & \dfrac{d}{\sqrt{Jg^{11}}} & c_2 g_{12} + c_3 g_{13} \\ 0 & c_3 J\sqrt{g^{11}} & c_2 g_{22} + c_3 g_{23} \\ 0 & -c_2 J\sqrt{g^{11}} & c_2 g_{32} + c_3 g_{33} \end{pmatrix}$$

$$c_2 = B^\theta/B, \quad c_2 = B^\phi/B$$

$$d = c_2(g_{23}g_{12} - g_{22}g_{31}) + c_3(g_{33}g_{12} - g_{32}g_{31})$$

$$g^{11} = (g_{22}g_{33} - g_{23}g_{32})/J^2$$

- **Dielectric Tensor in Non-Orthogonal Coordinates**:

$$\boxed{\overleftrightarrow{\epsilon} = \overleftrightarrow{\mu} \cdot \overleftrightarrow{\epsilon}_{sbh} \cdot \overleftrightarrow{\mu}^{-1}}$$

Fourier Mode Expansion

- **Fourier Expansion in Poloidal and Toroidal Directions**
- Spatial variation of wave electric field, medium and the L.H.S. of Maxwell's equation

$$E(\psi,\theta,\varphi) = \sum_{mn} E_{mn}(\psi) e^{\mathrm{i}(m\theta+n\varphi)}$$

$$G(\psi,\theta,\varphi) = \sum_{lk} G_{lk}(\psi) e^{\mathrm{i}(l\theta+kN_p\varphi)}$$

$$J(\boldsymbol{\nabla}\times\boldsymbol{\nabla}\times\boldsymbol{E}) = G(\psi,\theta,\varphi)E(\psi,\theta,\varphi) = \sum_{m'n'} [J(\boldsymbol{\nabla}\times\boldsymbol{\nabla}\times\boldsymbol{E})]_{m'n'} e^{\mathrm{i}(m'\theta+n'\varphi)}$$

- **Coupling between various modes** (N_h : Rotation number of helical coil in φ)

Mode Number	Toroidal Direcition	Poloidal Direction
Wave electric field $\boldsymbol{E}$	n	m
Medium G	kN_h	l
$J(\boldsymbol{\nabla}\times\boldsymbol{\nabla}\times\boldsymbol{E})$	n'	m'
Relations	$n' = n + kN_\mathrm{h}$	$m' = m + l$

Parallel Wave Number

- **Dielectric tensor** $\overleftrightarrow{\epsilon}(\psi, \theta, \varphi, k_\parallel^{m''n''})$ depends on **parallel wave number** $k_\parallel^{m'',n''}$ through the **plasma dispersion function** $Z[(\omega - N\omega_{\rm cs})/k_\parallel^{m''n''} v_{\rm Ts}]$

$$
\begin{aligned}
k_\parallel^{m'',n''} &= -i\hat{\boldsymbol{e}}_h \cdot \boldsymbol{\nabla} = -i\hat{\boldsymbol{e}}_h \cdot (\boldsymbol{\nabla}\theta \frac{\partial}{\partial\theta} + \boldsymbol{\nabla}\varphi \frac{\partial}{\partial\varphi}) \\
&= -i\hat{\boldsymbol{e}}_h \cdot (\boldsymbol{e}^2 \frac{\partial}{\partial\theta} + \boldsymbol{e}^3 \frac{\partial}{\partial\varphi}) = m'' \frac{B^\theta}{|B|} + n'' \frac{B^\varphi}{|B|}
\end{aligned}
$$

- **Fourier components of electric displacement**

$$
\begin{array}{ccccccccc}
(J \overleftrightarrow{\epsilon} \cdot \boldsymbol{E})^i & = & J \overleftrightarrow{g}^{-1} \cdot \overleftrightarrow{\mu} & \cdot & \overleftrightarrow{\epsilon}_{sbh} & \cdot & \overleftrightarrow{\mu}^{-1} & \cdot & \boldsymbol{E}_i \\
m' & & \ell_3 & & \ell_2 & & \ell_1 & & m \\
n' & & k_3 & & k_2 & & k_1 & & n
\end{array}
$$

therefore

$$
\begin{aligned}
m'' &= m + \ell_1 + \frac{1}{2}\ell_2 \qquad & n'' &= n + k_1 + \frac{1}{2}k_2 \\
m' &= m + \ell_1 + \ell_2 + \ell_2 \qquad & n' &= n + k_1 + k_2 + k_3
\end{aligned}
$$

Destabilization by Energetic Ion

- **Drift kinetic equation**

$$\left[\frac{\partial}{\partial t} + v_\parallel \nabla_\parallel + (\boldsymbol{v}_\mathrm{d} + \boldsymbol{v}_\mathrm{E}) \cdot \boldsymbol{\nabla} + \frac{e_\alpha}{m_\alpha}(v_\parallel E_\parallel + \boldsymbol{v}_\mathrm{d} \cdot \boldsymbol{E})\frac{\partial}{\partial \varepsilon}\right] f_\alpha = 0$$

where

$$\varepsilon = \frac{1}{2} m_\alpha v^2, \quad \boldsymbol{v}_\mathrm{E} = \frac{\boldsymbol{E} \times \boldsymbol{B}}{B^2}, \quad \boldsymbol{v}_\mathrm{d} = v_\mathrm{d} \sin\theta \hat{\boldsymbol{r}} + v_\mathrm{d} \cos\theta \hat{\boldsymbol{\theta}}, \quad v_\mathrm{d} = \frac{m_\alpha}{e_\alpha B R} \cdot \frac{v_\perp^2}{2 + v_\parallel^2}$$

- **Anti-Hermite part of electric susceptibility tensor**

$$\begin{aligned}
\overleftrightarrow{\chi}_{mm'} = & \begin{pmatrix} 1 & -\mathrm{i} & 0 \\ -\mathrm{i} & -1 & 0 \\ 0 & 0 & 0 \end{pmatrix} P_{m-1,m-2} \delta_{m',m-2} \\
& + \begin{pmatrix} 0 & 0 & Q_{m-1,m-1} \\ 0 & 0 & -\mathrm{i}\, Q_{m-1,m-1} \\ Q_{m,m-1} & -\mathrm{i}\, Q_{m,m-1} & 0 \end{pmatrix} \delta_{m',m-1} \\
& + \begin{pmatrix} (P_{m-1,m} + P_{m+1,m}) & \mathrm{i}\,(P_{m-1,m} - P_{m+1,m}) & 0 \\ -\mathrm{i}\,(P_{m-1,m} - P_{m+1,m}) & (P_{m-1,m} + P_{m+1,m}) & 0 \\ 0 & 0 & R_{m-1,m-1} \end{pmatrix} \delta_{m',m}
\end{aligned}$$

$$
+ \begin{pmatrix} 0 & 0 & Q_{m+1,m+1} \\ 0 & 0 & \mathrm{i}\, Q_{m+1,m+1} \\ Q_{m,m+1} & \mathrm{i}\, Q_{m,m+1} & 0 \end{pmatrix} \delta_{m',m+1}
$$

$$
+ \begin{pmatrix} 1 & \mathrm{i} & 0 \\ \mathrm{i} & -1 & 0 \\ 0 & 0 & 0 \end{pmatrix} P_{m+1,m+2} \delta_{m',m+2}
$$

- **In the case of Maxwellean velocity distributution**

$$
\begin{aligned}
P_{m,m'} &= \mathrm{i}\, \frac{\omega_{\mathrm{p}\alpha}^2}{2\omega^2} \left(1 - \frac{\omega_{*\alpha m'}}{\omega}\right) \frac{\rho_\alpha^2}{R^2} \sqrt{\pi} x_m \left(\frac{1}{2} + x_m^2 + x_m^4\right) \mathrm{e}^{-x_m^2} \\
Q_{m,m'} &= \mathrm{i}\, \frac{\omega_{\mathrm{p}\alpha}^2}{2\omega^2} \left(1 - \frac{\omega_{*\alpha m'}}{\omega}\right) \frac{\rho_\alpha}{R} \sqrt{\pi} 2 x_m^2 \left(\frac{1}{2} + x_m^2\right) \mathrm{e}^{-x_m^2} \\
R_{m,m'} &= \mathrm{i}\, \frac{\omega_{\mathrm{p}\alpha}^2}{2\omega^2} \left(1 - \frac{\omega_{*\alpha m'}}{\omega}\right) \sqrt{\pi} 4 x_m^3 \mathrm{e}^{-x_m^2} \\
x_m &= \omega / |k_{\parallel m}| v_{\mathrm{T}\alpha}, \\
\rho_\alpha &= v_{\mathrm{T}\alpha} / \omega_{\mathrm{c}\alpha}, \\
v_{\mathrm{T}\alpha} &= \sqrt{2 T_\alpha / m_\alpha}
\end{aligned}
$$

ICRF Waves in Toroidal Helical Plasmas (Cold Plasma Model)

LHD ($B_0 = 3\,\mathrm{T}$, $R_0 = 3.8\,\mathrm{m}$)

$f = 42\,\mathrm{MHz}$, $n_{\phi 0} = 20$, $n_{\mathrm{e}0} = 3 \times 10^{19}\,\mathrm{m}^{-3}$, $n_{\mathrm{H}}/(n_{\mathrm{He}} + n_{\mathrm{H}}) = 0.235$,

$N_{\mathrm{rmax}} = 100$, $N_{\theta\mathrm{max}} = 16$ $(m = -7 \ldots 7)$, $N_{\phi\mathrm{max}} = 4$ $(n = 10, 20, 30)$

Wave electric field (imaginary part of poloidal component)

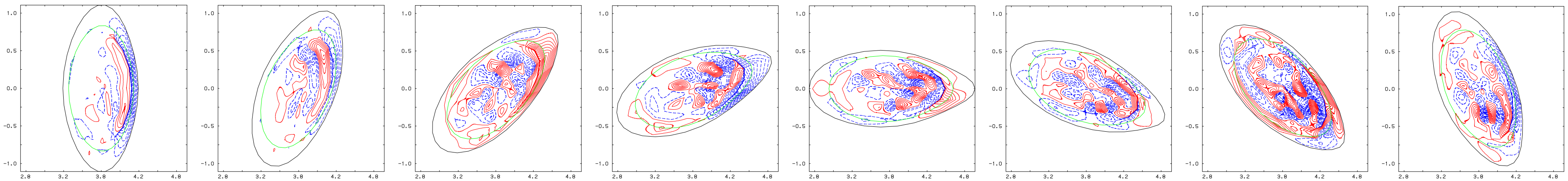

Power deposition profile (minority ion)

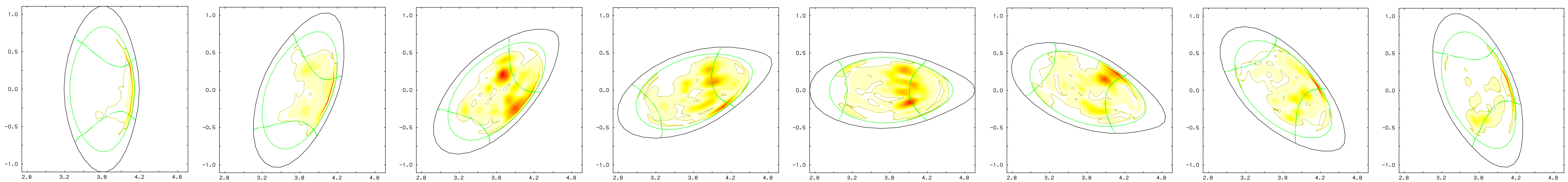

Typical Poloidal Profile

LHD ($B_0 = 3\,\mathrm{T}$, $R_0 = 3.8\,\mathrm{m}$)

$f = 42\,\mathrm{MHz}$, $n_{\phi 0} = 20$, $n_{e0} = 3 \times 10^{19}\,\mathrm{m}^{-3}$, $n_{\mathrm{H}}/(n_{\mathrm{He}} + n_{\mathrm{H}}) = 0.235$,

$N_{\mathrm{rmax}} = 100$, $N_{\theta\mathrm{max}} = 16$ ($m = -7 \ldots 7$), $N_{\phi\mathrm{max}} = 4$ ($n = 10, 20, 30$)

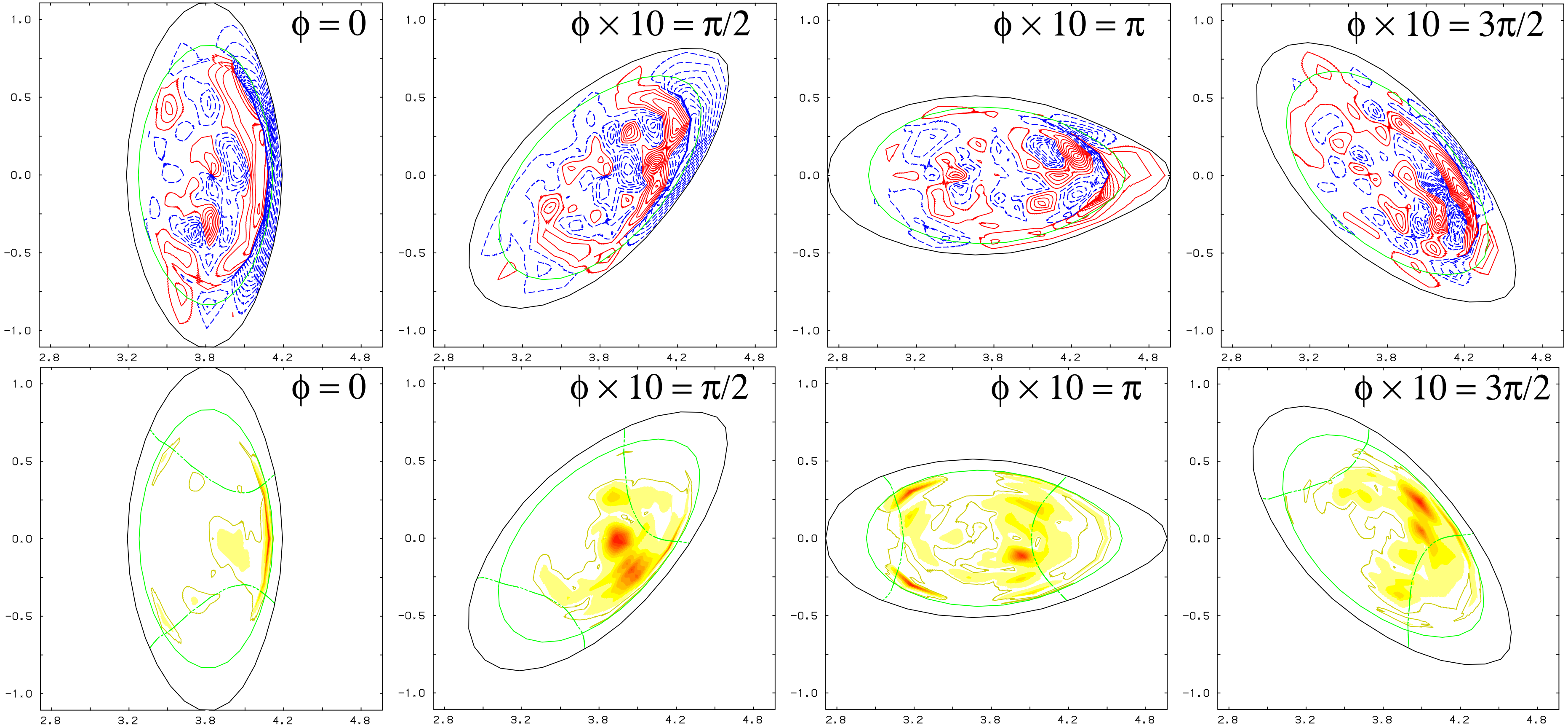

Frequency Dependence

- **Power deposition profile**

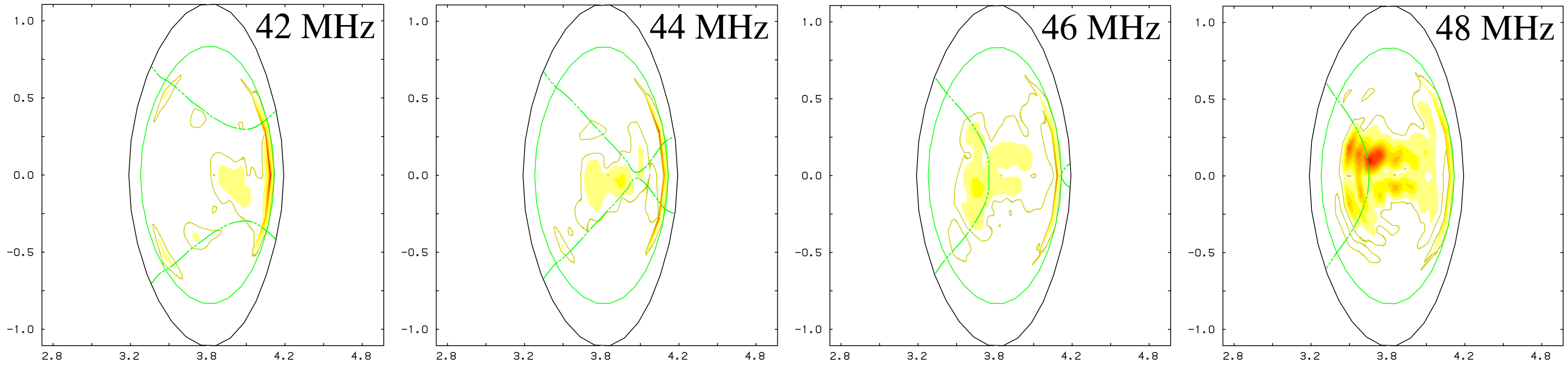

- **Radial deposition profile**

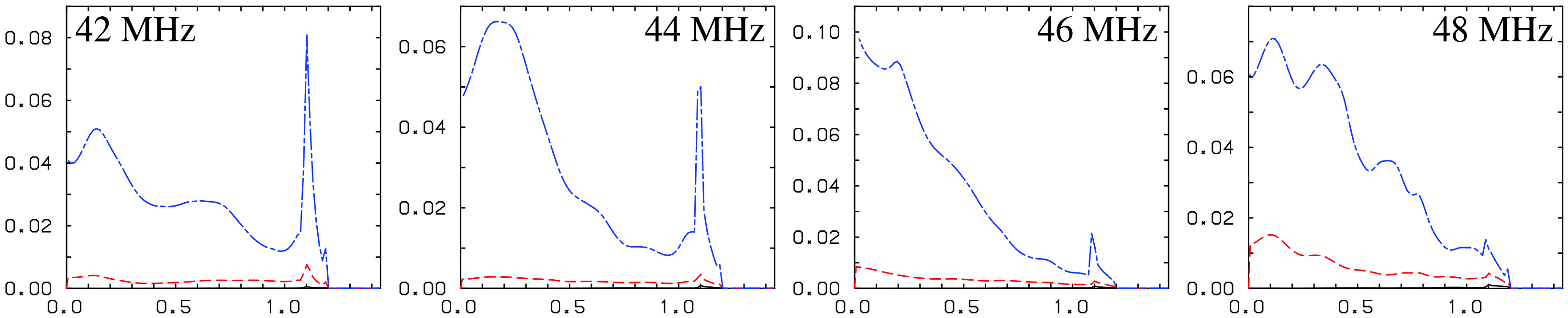

- **Total power absorption**

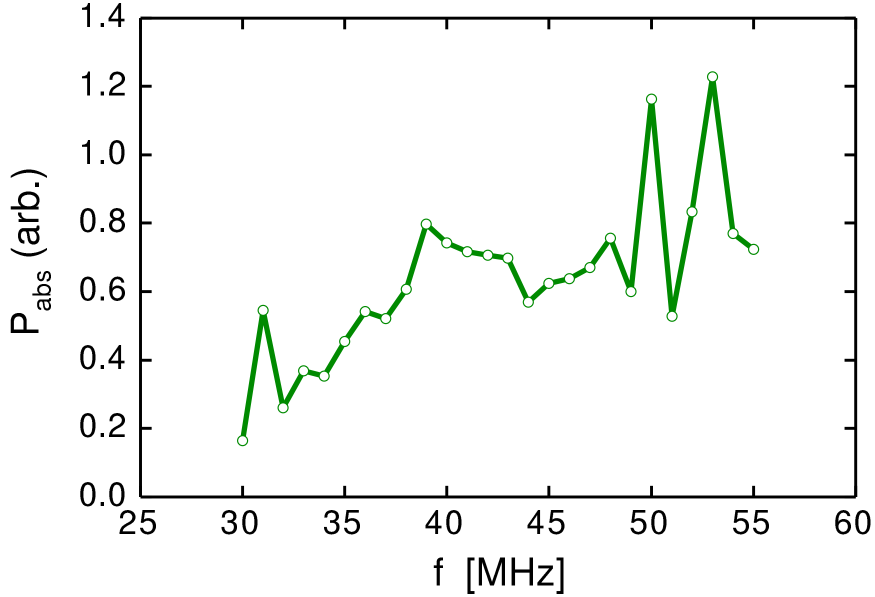

Parameter Dependence

Dependence on n_{H} Ratio

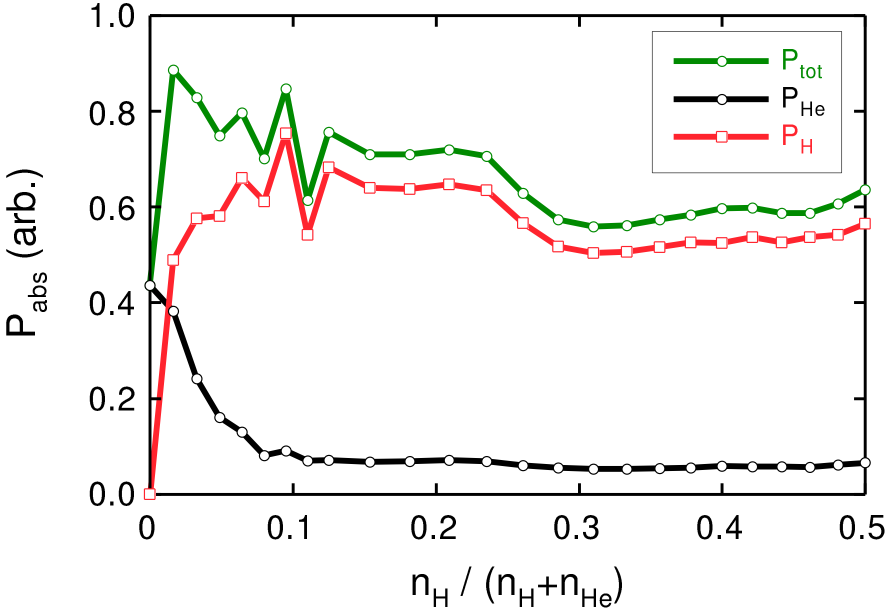

Dependence on $n_{\phi 0}$

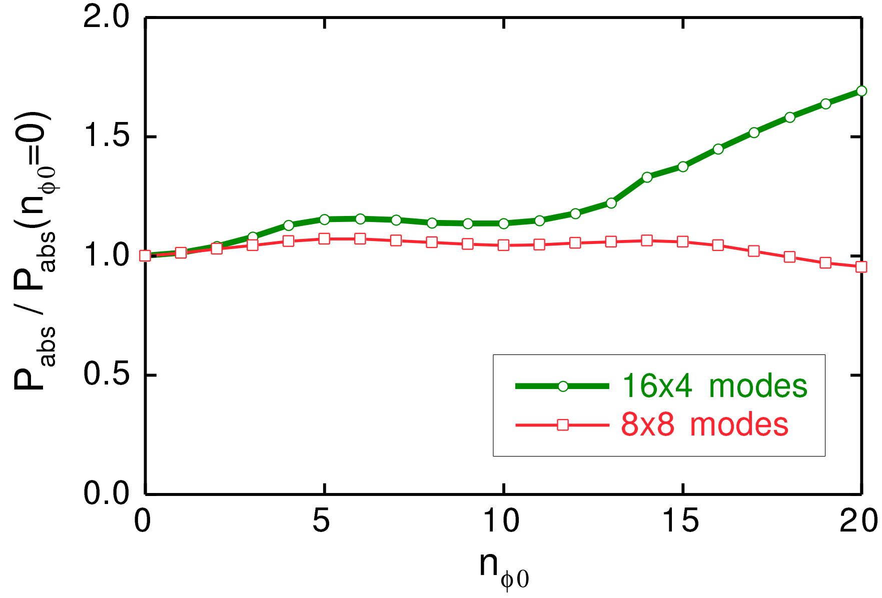

Effect of Toroidal Plasma Rotation

Experimental Results on JT-60U

Ref. M. Saigusa et al., Nucl. Fusion, 37 (1997) 1559.

Co-NBI ⟶ Counter-NBI

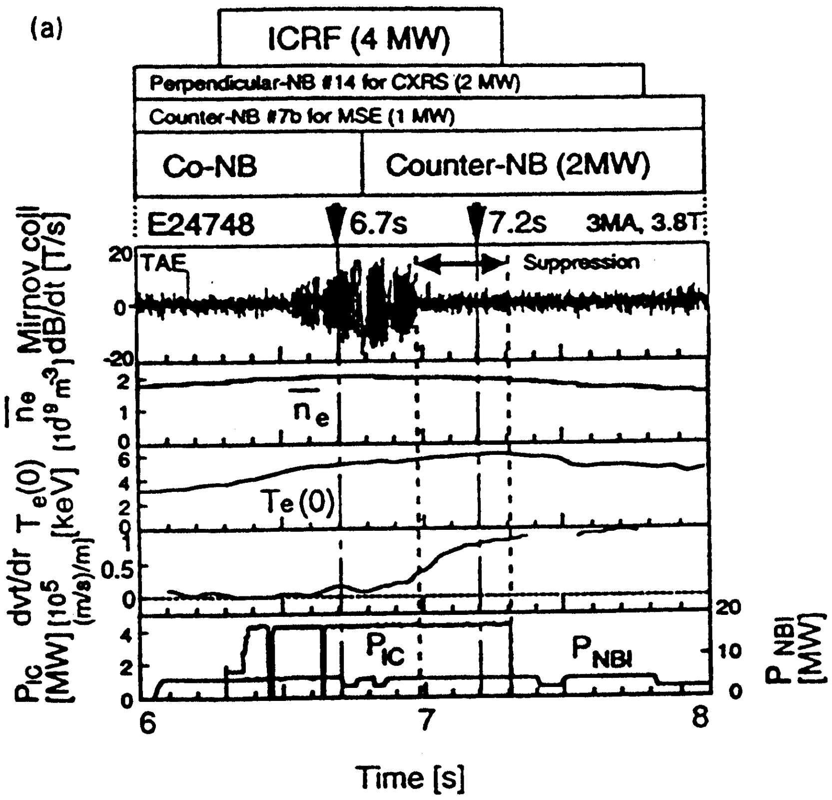

Counter-NBI: stabilization

Counter-NBI ⟶ Co-NBI

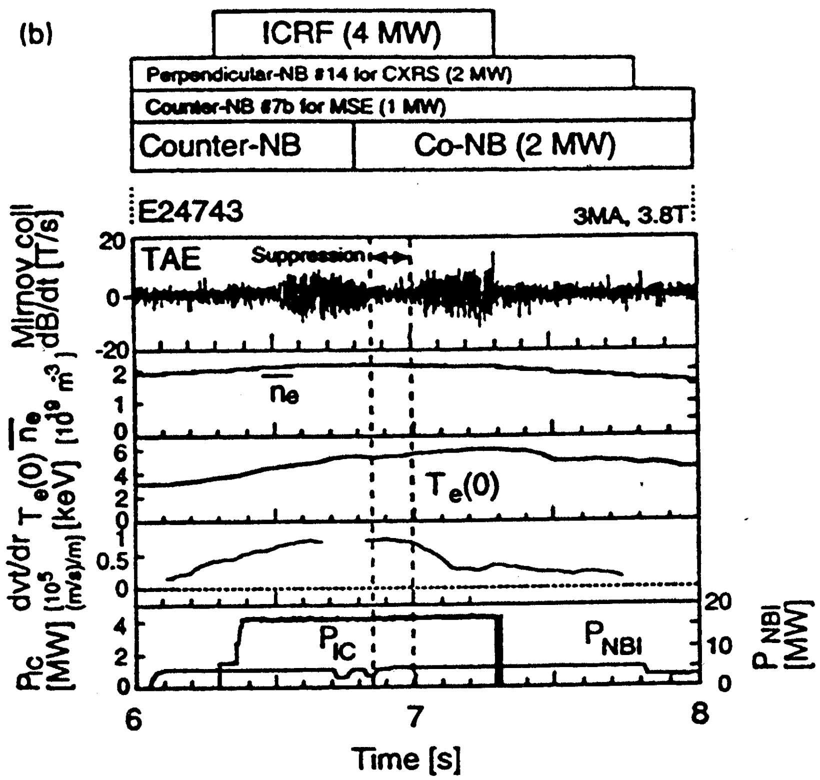

Co-NBI: destabilization

Dispersion Relation including Toroidal Rotation

- **Dispersion relation**

$$\left({k_{||m}}^2-\frac{(\omega-k_{||m}u)^2}{{v_\mathrm{A}}^2}\right)\left({k_{||m+1}}^2-\frac{(\omega-k_{||m+1}u)^2}{{v_\mathrm{A}}^2}\right)-\epsilon^2\frac{(\omega-k_{||m}u)^2(\omega-k_{||m+1}u)^2}{{v_\mathrm{A}}^4}=0$$

- Parallel wave number $k_{||m}=\dfrac{1}{R}\left(n+\dfrac{m}{q}\right)$
- Alfvén resonance condition without toroidal effect

$$\omega^2={k_{||m}}^2(u\pm v_\mathrm{A})^2, \qquad \omega^2={k_{||m+1}}^2(u\pm v_\mathrm{A})^2$$

- Condition for frequency gap

$$k_{||m}\left(u-v_\mathrm{A}\right)=k_{||m+1}(u+v_\mathrm{A}\right)$$

- **Safety factor at TAE gap**: q

$$q=-\frac{m+1/2}{n}-\frac{1}{2n}\frac{u}{v_\mathrm{A}}$$

- **TAE gap frequency** ω: parabolic with respect to u

$$\omega=\frac{v_\mathrm{A}}{2qR}(1-\frac{u^2}{{v_\mathrm{A}}^2})$$

Effect of Rotation on $n = 7$ mode

- $n = 7$, $m = -17 \sim -3$, $f = 223\,\mathrm{kHz}$

Shape of eigen function agree with Nova-K

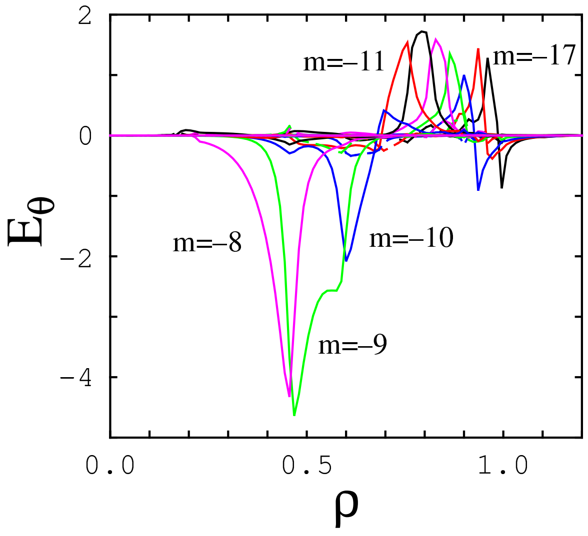

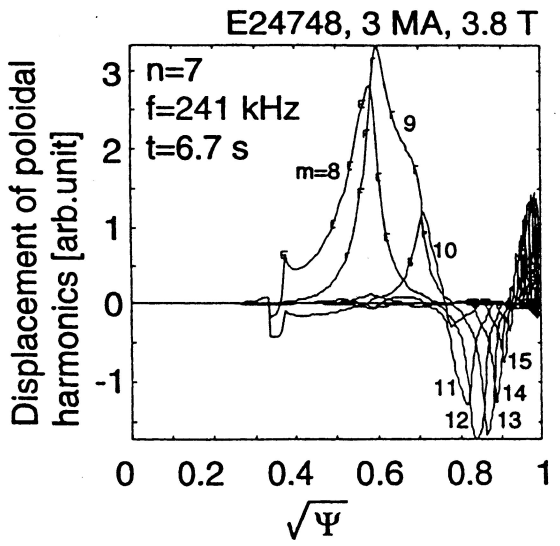

- Rotation velocity dependence: Stabilizing for co rotation (Contradict with exp.)

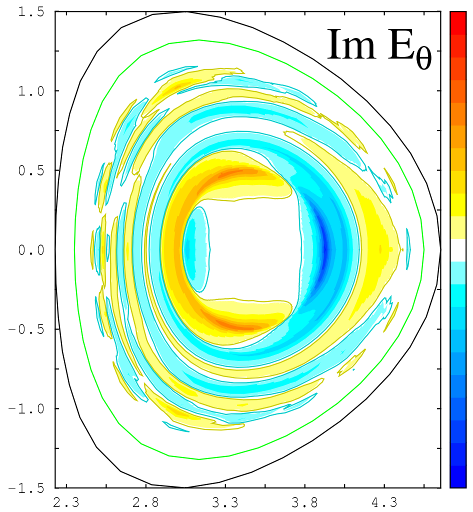

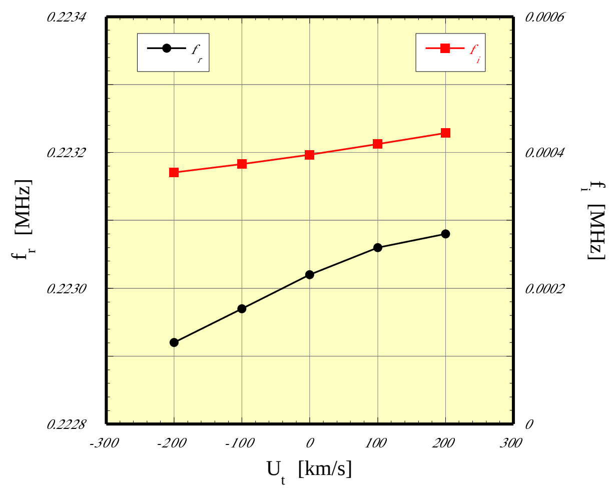

Influence of poloidal mode range : $n = 7$ mode

- Radial structure of Alfvén Continuum

$m = -17 \sim -3$

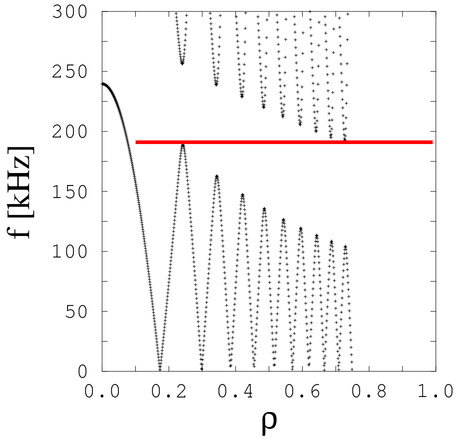

$m = -21 \sim -7$

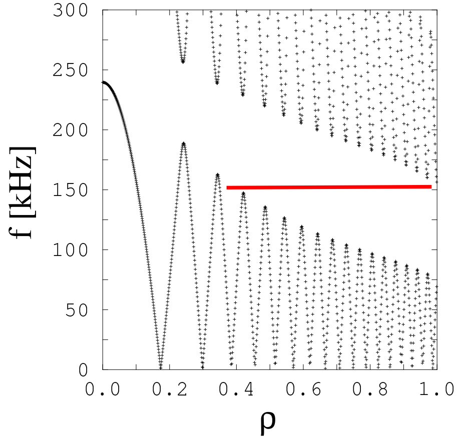

- $n = 7$, $m = -21 \sim -7$, $f = 238\,\text{kHz}$: Destabilizing for co-rotation (agree with exp.)

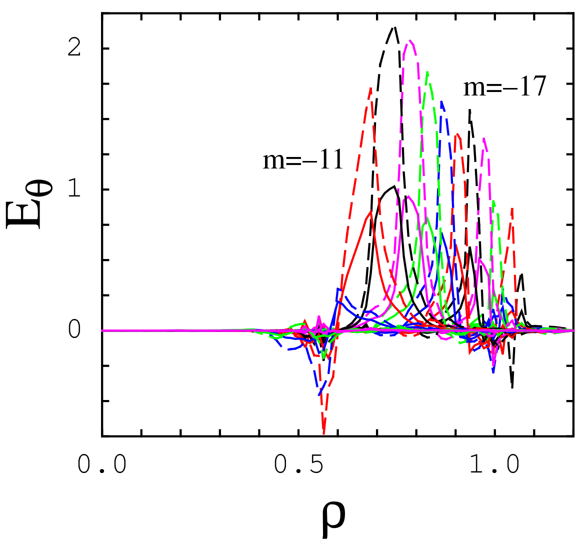

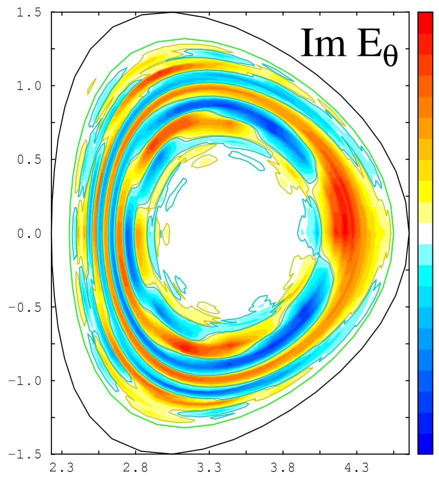

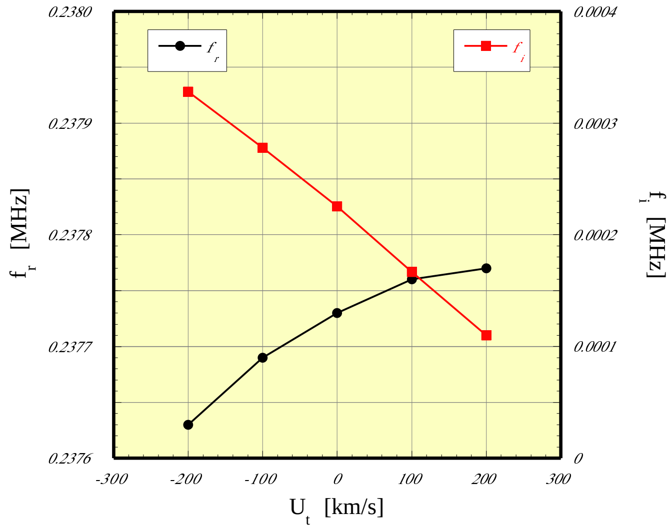

Alfvén Eigenmodes Below Gap requency

Parameters

R	3.5016 m
a	0.9837 m
κ	.2810
δ	0.3098
b/a	1.1
B_0	3.3119 T
I_p	1.6945 MA
$n_e(0)$	0.2356 $10^{20}m^{-3}$
$n_e(a)$	0.05 $10^{20}m^{-3}$
$T_e(0)$	4.1 keV
$T_e(a)$	0.8 keV
$T_D(0)$	3.7 keV
$T_D(a)$	0.4 keV

Radial profile of Alfvén resonance frequency

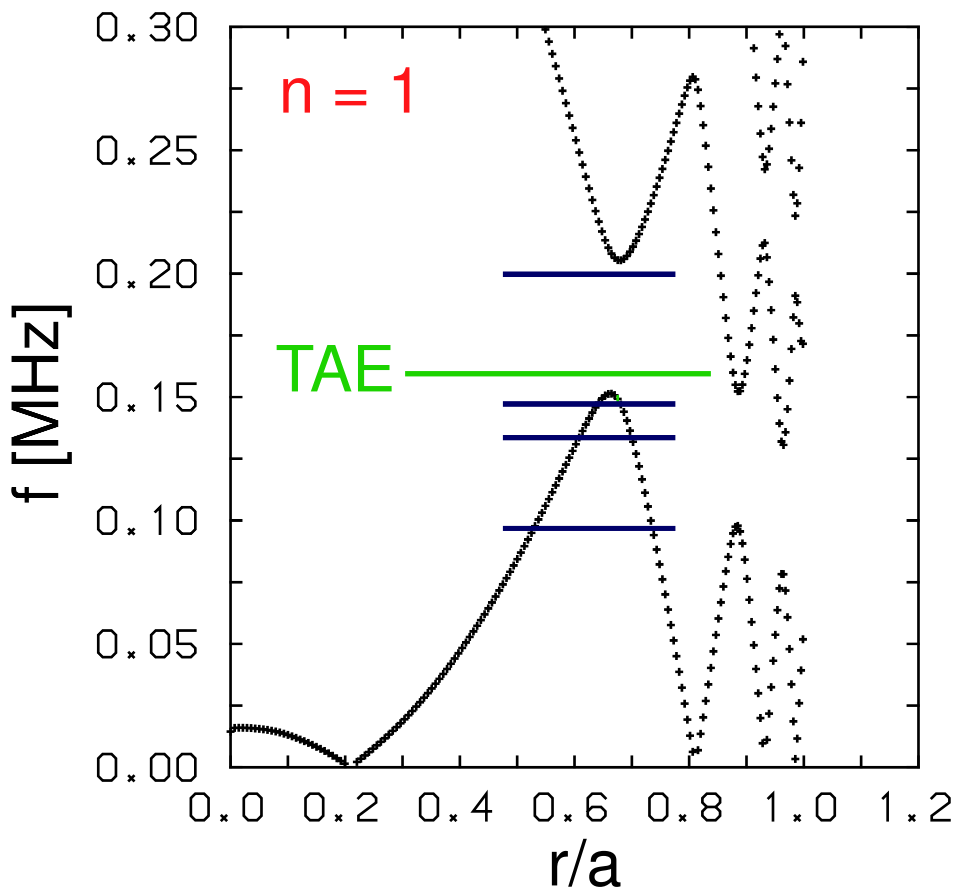

Complex Eigen Frequency of Alfvén Eigenmode

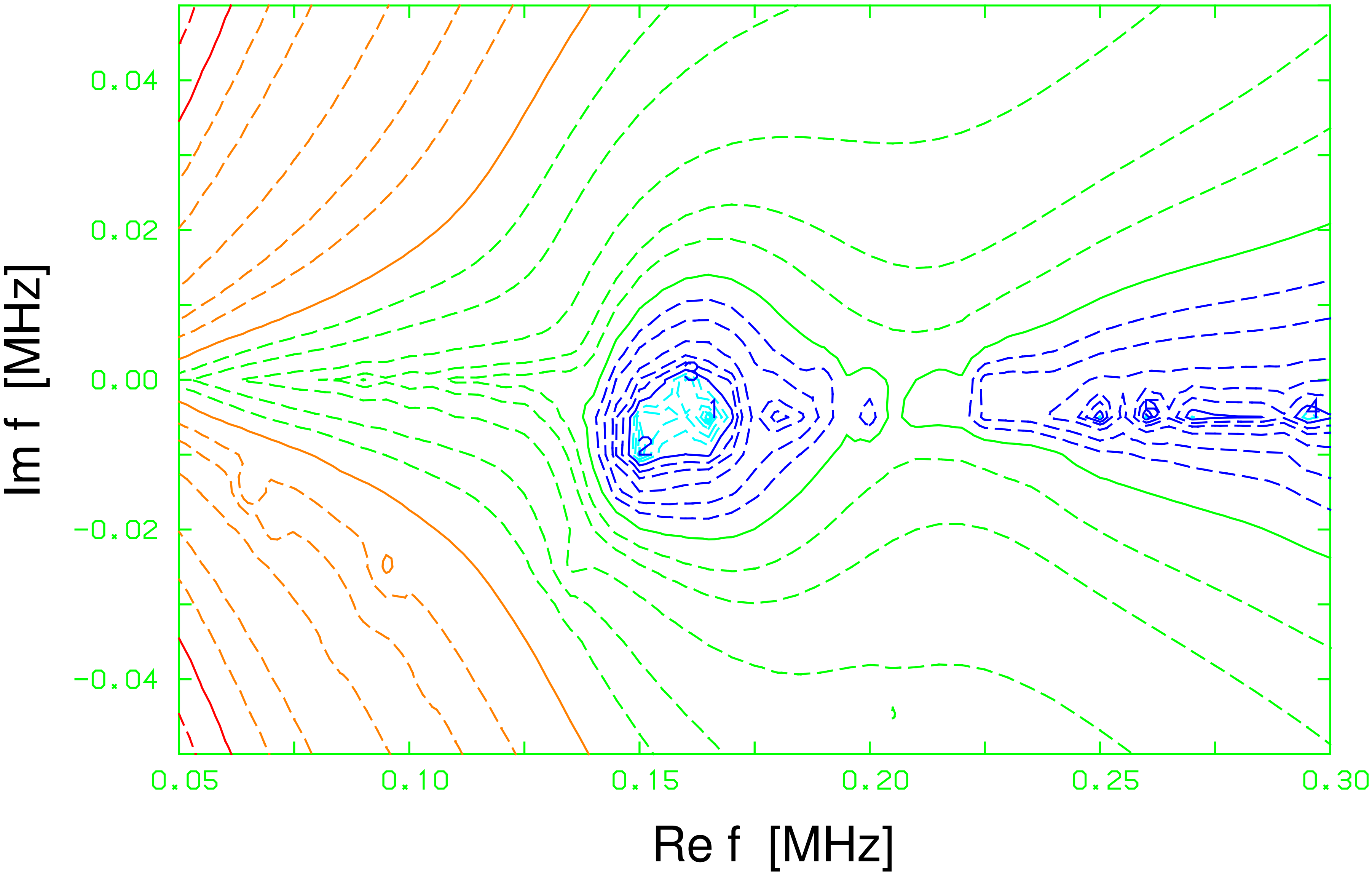

Radial Mode Structure of Alfvén Eigenmode ($n = 1$)

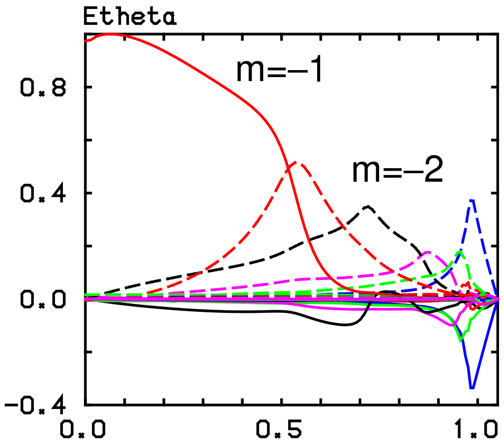

$f_{\mathrm{r}} = 97.0\,\mathrm{kHz}$

$f_{\mathrm{i}} = -23.6\,\mathrm{kHz}$

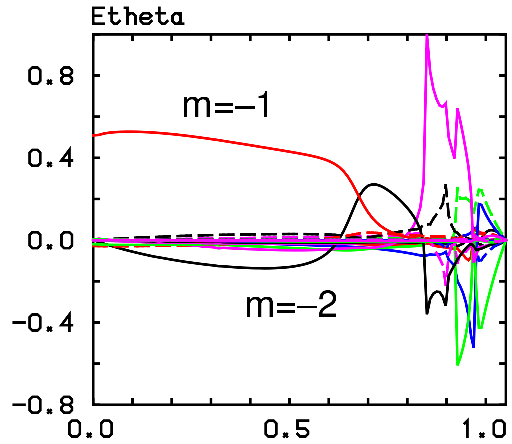

$f_{\mathrm{r}} = 199.4\,\mathrm{kHz}$

$f_{\mathrm{i}} = -3.37\,\mathrm{kHz}$

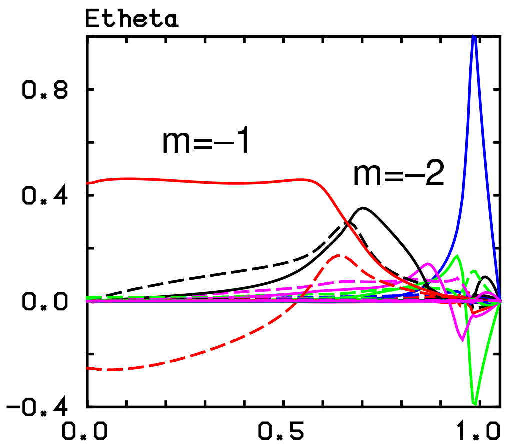

$f_{\mathrm{r}} = 136.4\,\mathrm{kHz}$

$f_{\mathrm{i}} = -24.1\,\mathrm{kHz}$

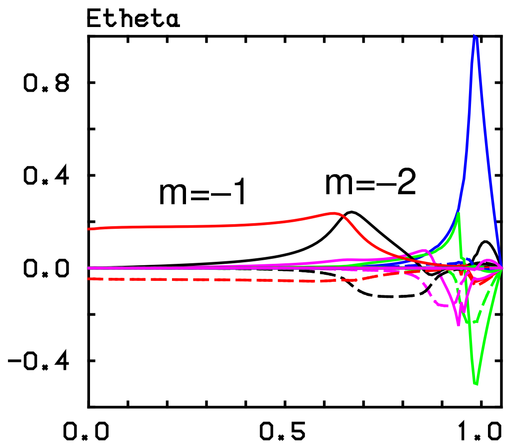

$f_{\mathrm{r}} = 149.8\,\mathrm{kHz}$

$f_{\mathrm{i}} = -8.12\,\mathrm{kHz}$

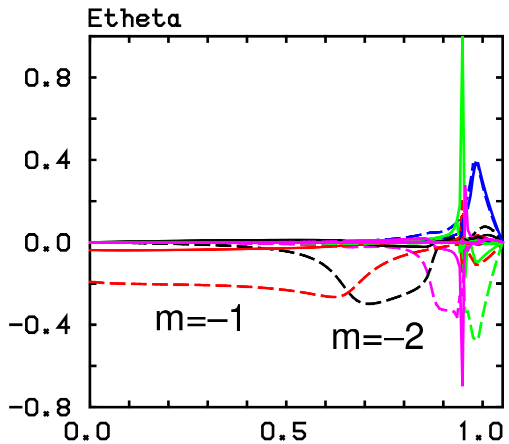

$f_{\mathrm{r}} = 164.3\,\mathrm{kHz}$

$f_{\mathrm{i}} = -5.08\,\mathrm{kHz}$

Mode Structure with Energetic Particle

- $n_{\mathrm{F0}} = 2 \times 10^{17}\,\mathrm{m}^{-3}$, $T_{\mathrm{B}} = 500\,\mathrm{keV}$, $L_{n\mathrm{B}} = 0.5\,\mathrm{m}$

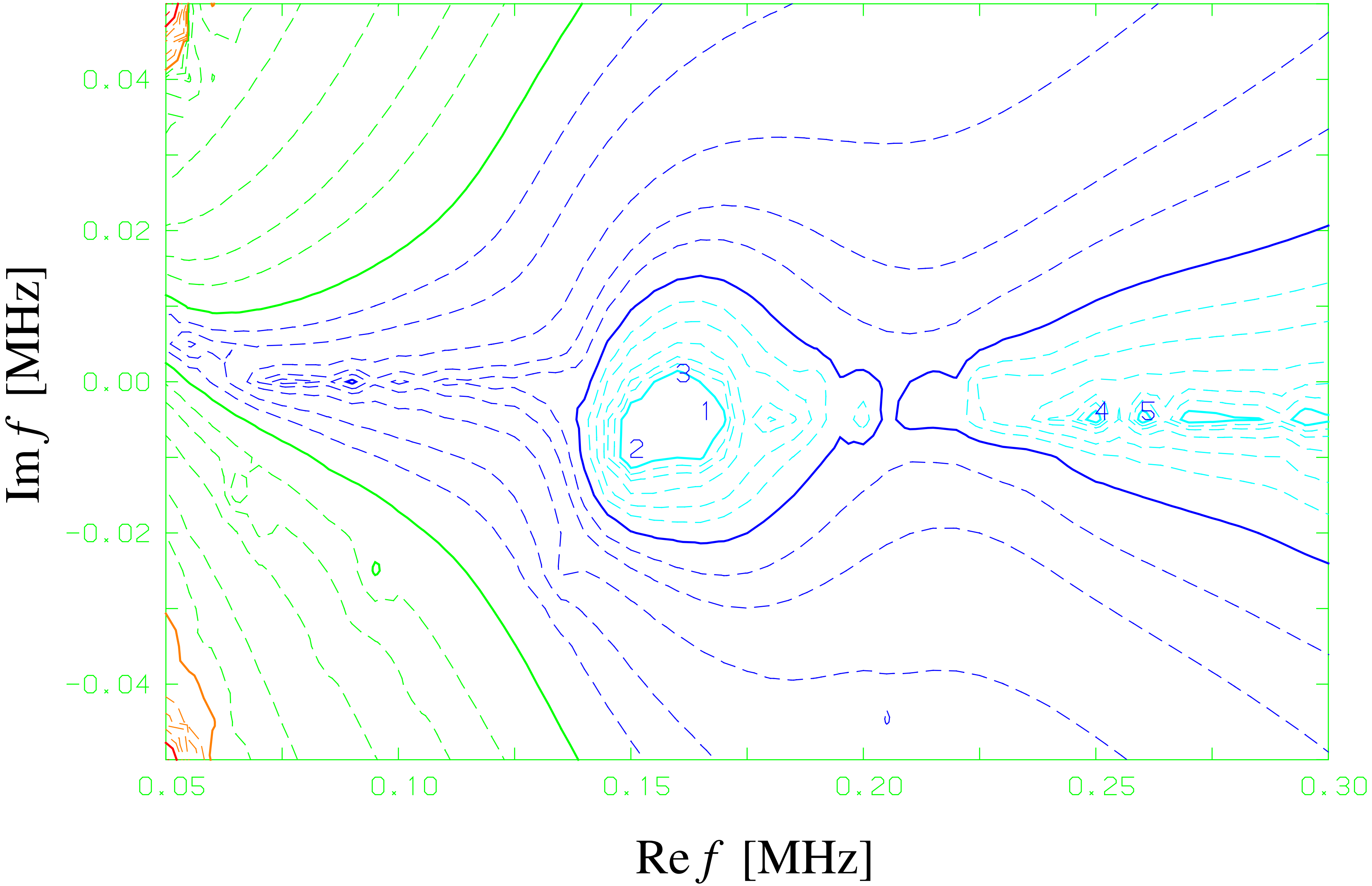

Modes and Eigenfunctions Driven by Energetic Ions

- $n_{\mathrm{F0}} = 2\times10^{17}\,\mathrm{m}^{-3}$, $T_{\mathrm{F}} = 500\,\mathrm{keV}$, $L_{n\mathrm{F}} = 0.5\,\mathrm{m}$, $n = 1$

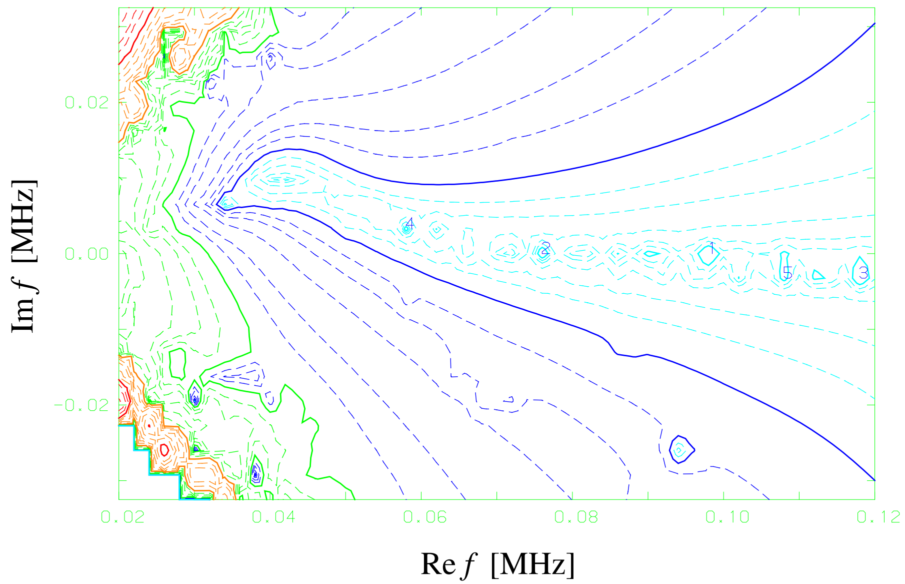

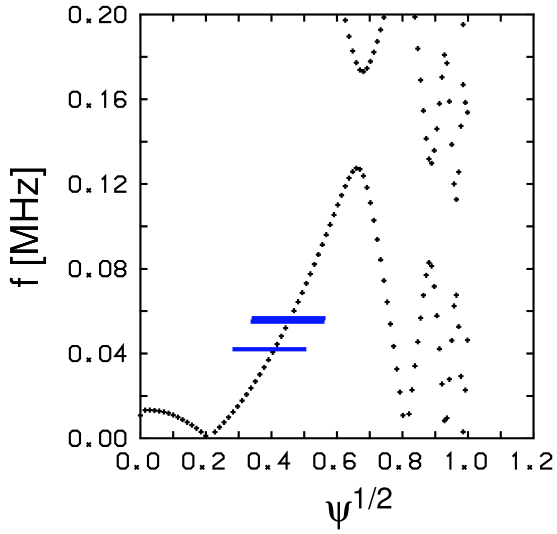

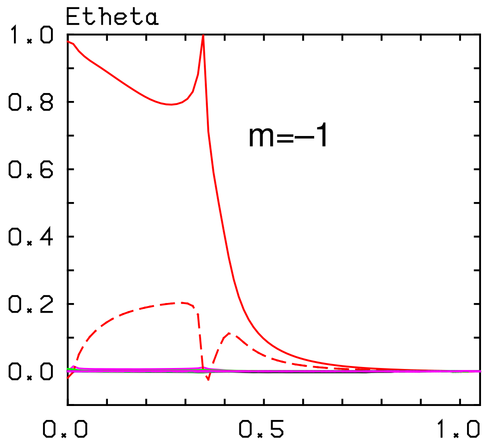

$f_{\mathrm{r}} = 41.8\,\mathrm{kHz}$

$f_{\mathrm{i}} = 8.1\,\mathrm{kHz}$

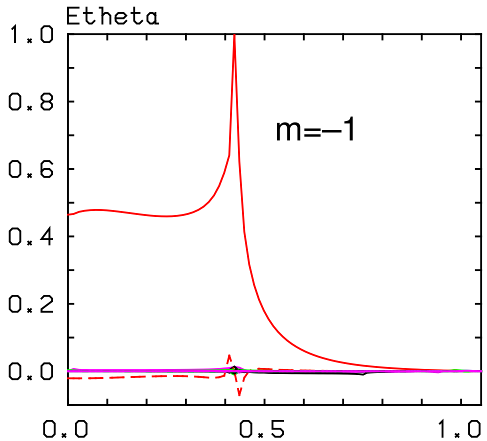

$f_{\mathrm{r}} = 57.7\,\mathrm{kHz}$

$f_{\mathrm{i}} = 3.6\,\mathrm{kHz}$

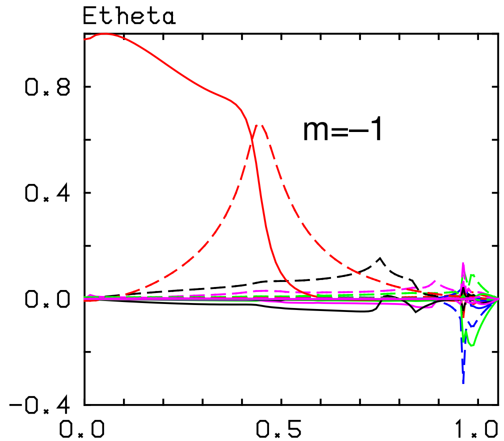

$f_{\mathrm{r}} = 58.0\,\mathrm{kHz}$

$f_{\mathrm{i}} = -6.0\,\mathrm{kHz}$

Parameter Dependence of Mode Structure

$n_{\rm F0} = 0 \times 10^{17}\,{\rm m}^{-3}$, $T_{\rm B} = 0.5\,{\rm MeV}$

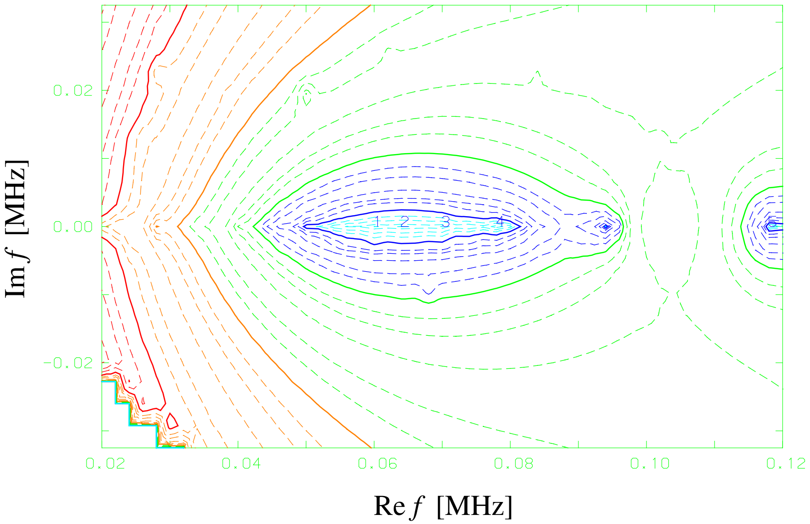

$n_{\rm F0} = 1 \times 10^{17}\,{\rm m}^{-3}$, $T_{\rm B} = 0.5\,{\rm MeV}$

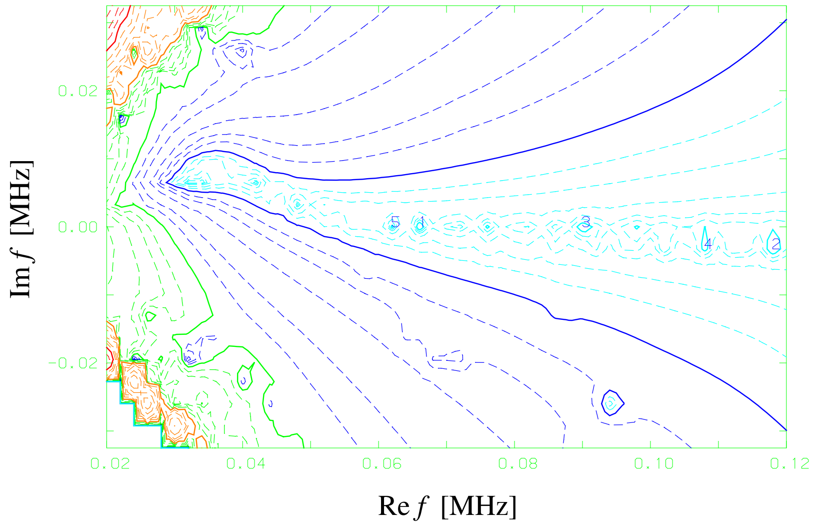

$n_{\rm F0} = 3 \times 10^{17}\,{\rm m}^{-3}$, $T_{\rm B} = 0.5\,{\rm MeV}$

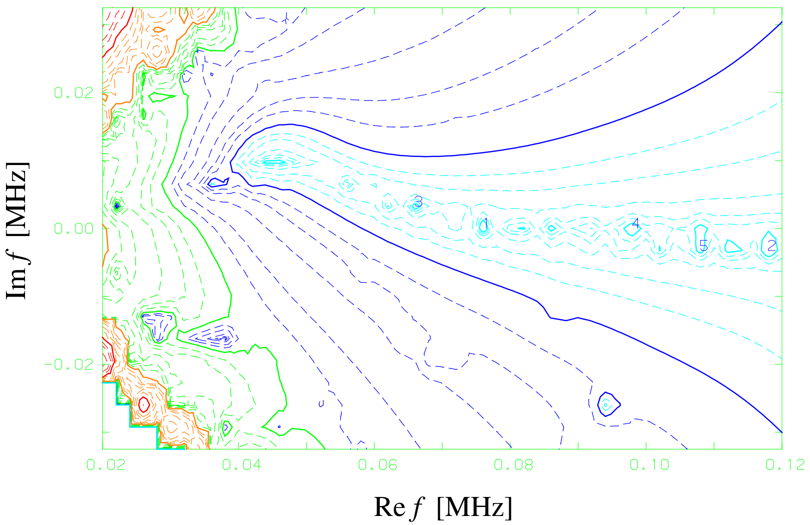

$n_{\rm F0} = 1 \times 10^{17}\,{\rm m}^{-3}$, $T_{\rm B} = 1\,{\rm MeV}$

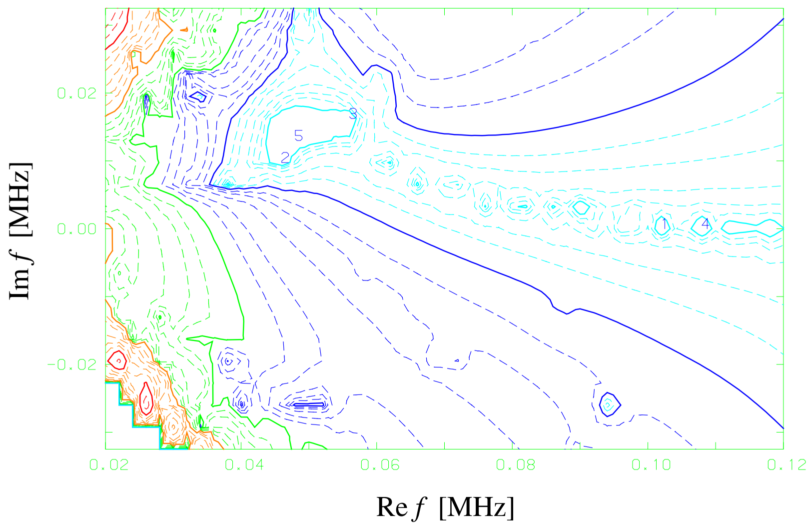

Analysis of TAE in Reversed Shear Configuration

Assumed q profile

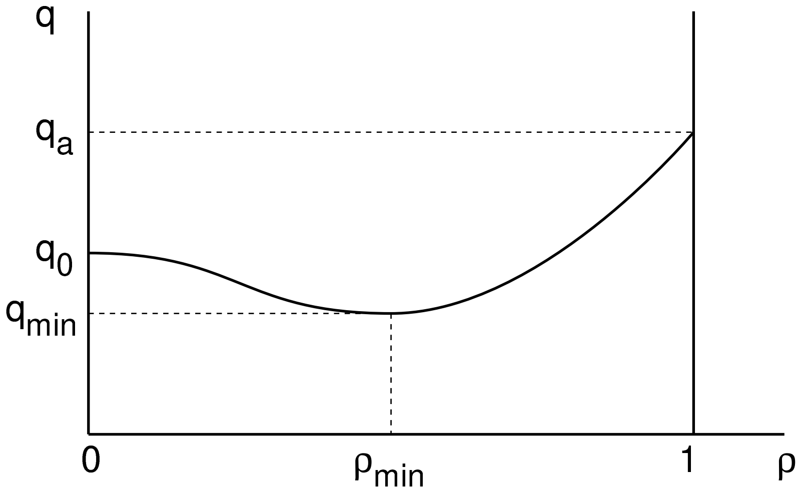

Plasma Parameters

Major Radius	R_0	$3\,\mathrm{m}$
Minor Radius	a	$1\,\mathrm{m}$
Wall Radius	b	$1.2\,\mathrm{m}$
Toroidal Magnetic Field	B_0	$3\,\mathrm{T}$
Center Electron Density	$n_e(0)$	$10^{20}\,\mathrm{m}^{-3}$
Edge Electron Density	$n_e(a)$	$10^{20}\,\mathrm{m}^{-3}$
Central Temperature	$T(0)$	$3\,\mathrm{keV}$
Edge Temperature	$T(a)$	$3\,\mathrm{keV}$
Ion Species		Deuterium
Central Safety Factor	$q(0)$	3
Edge Safety Factor	$q(a)$	5
Toroidal Mode Number	n	1
q-Minimum Radius	$\rho_{\min}$	0.5

$q_{\min}$ Dependence of Alfvén Frequency Profile

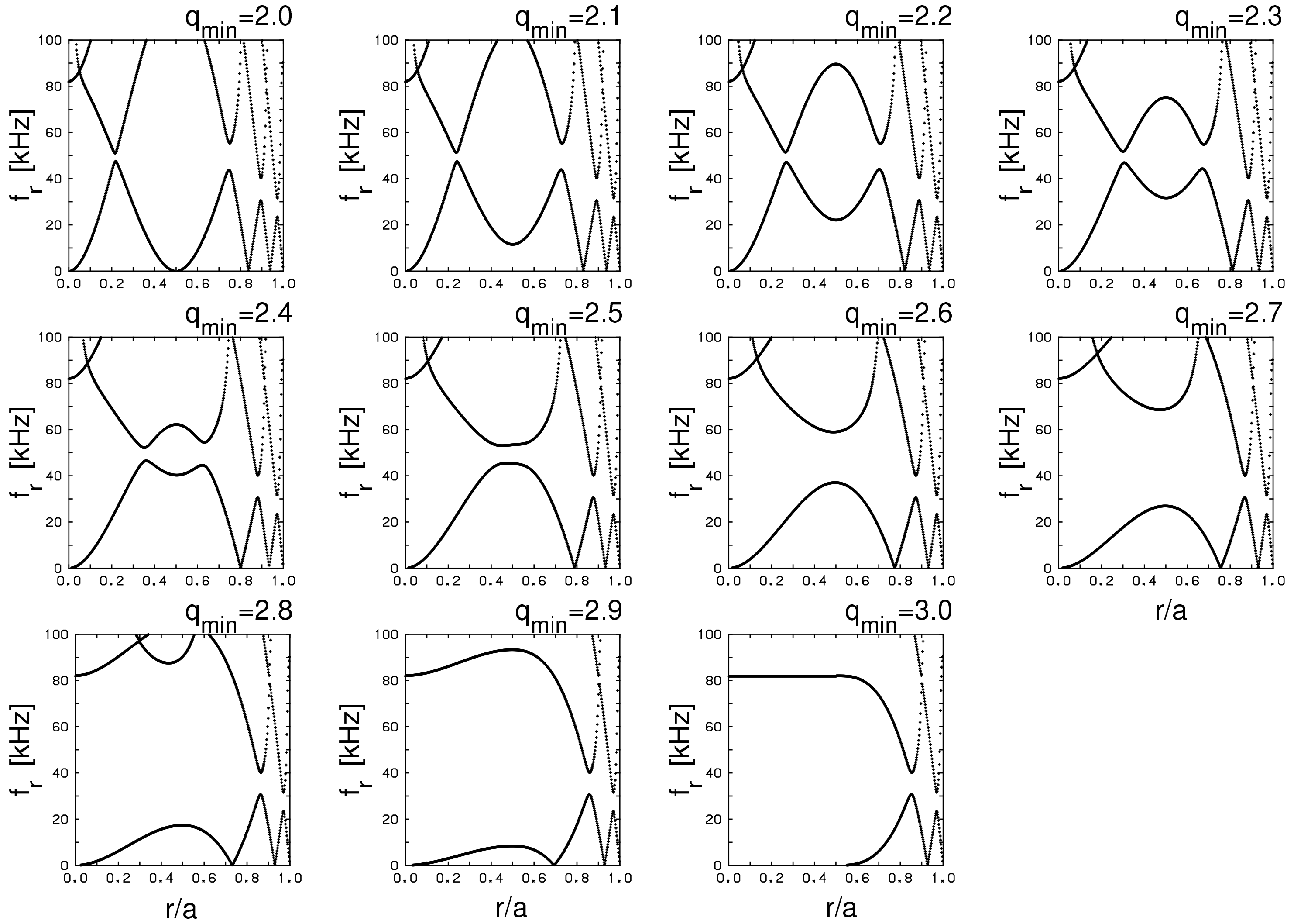

$q_{\min}$ Dependence of Eigen Frequency and Damping Rate

Eigen Frequency

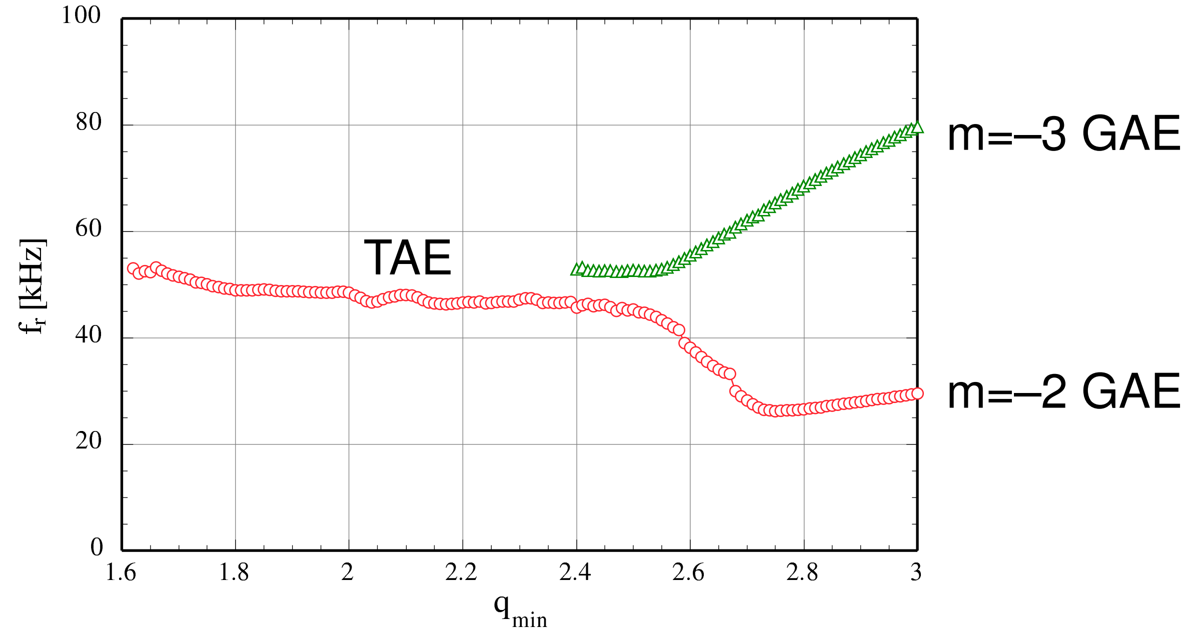

−Damping Rate

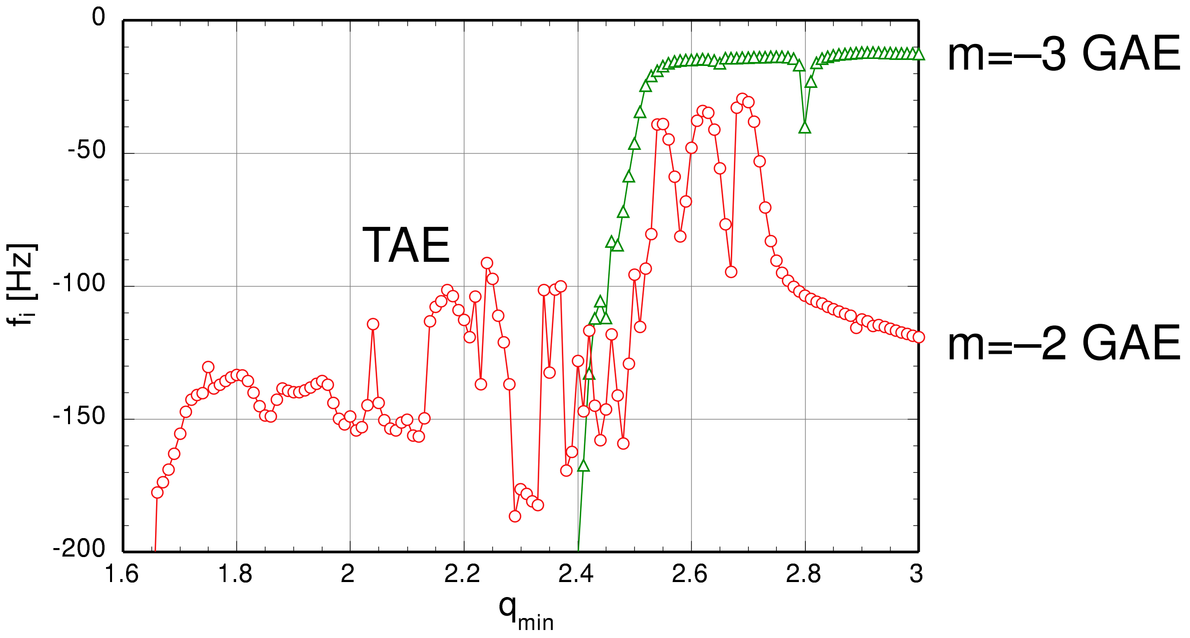

Effect of ITB Density Profile on TAE

Density profile

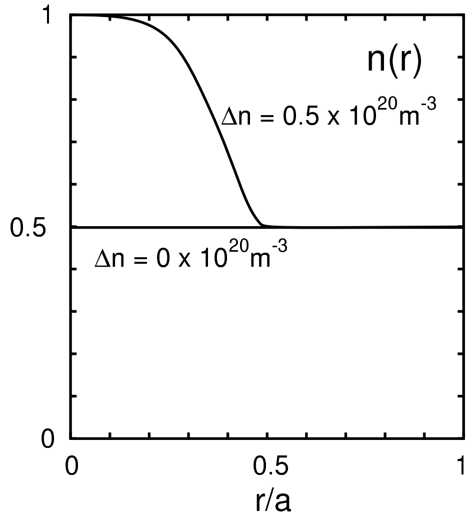

q profile

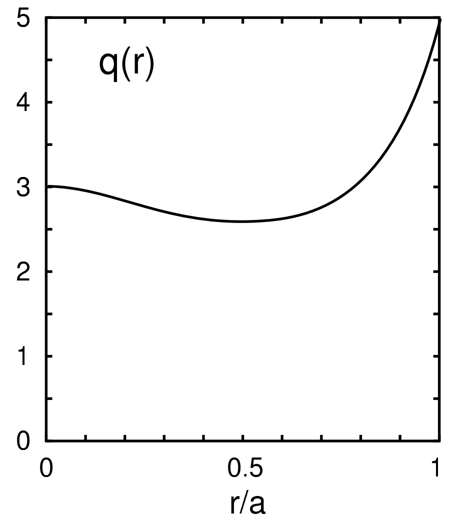

Alfvén resonance frequency

$q_{\min} = 2.5$

$q_{\min} = 2.6$

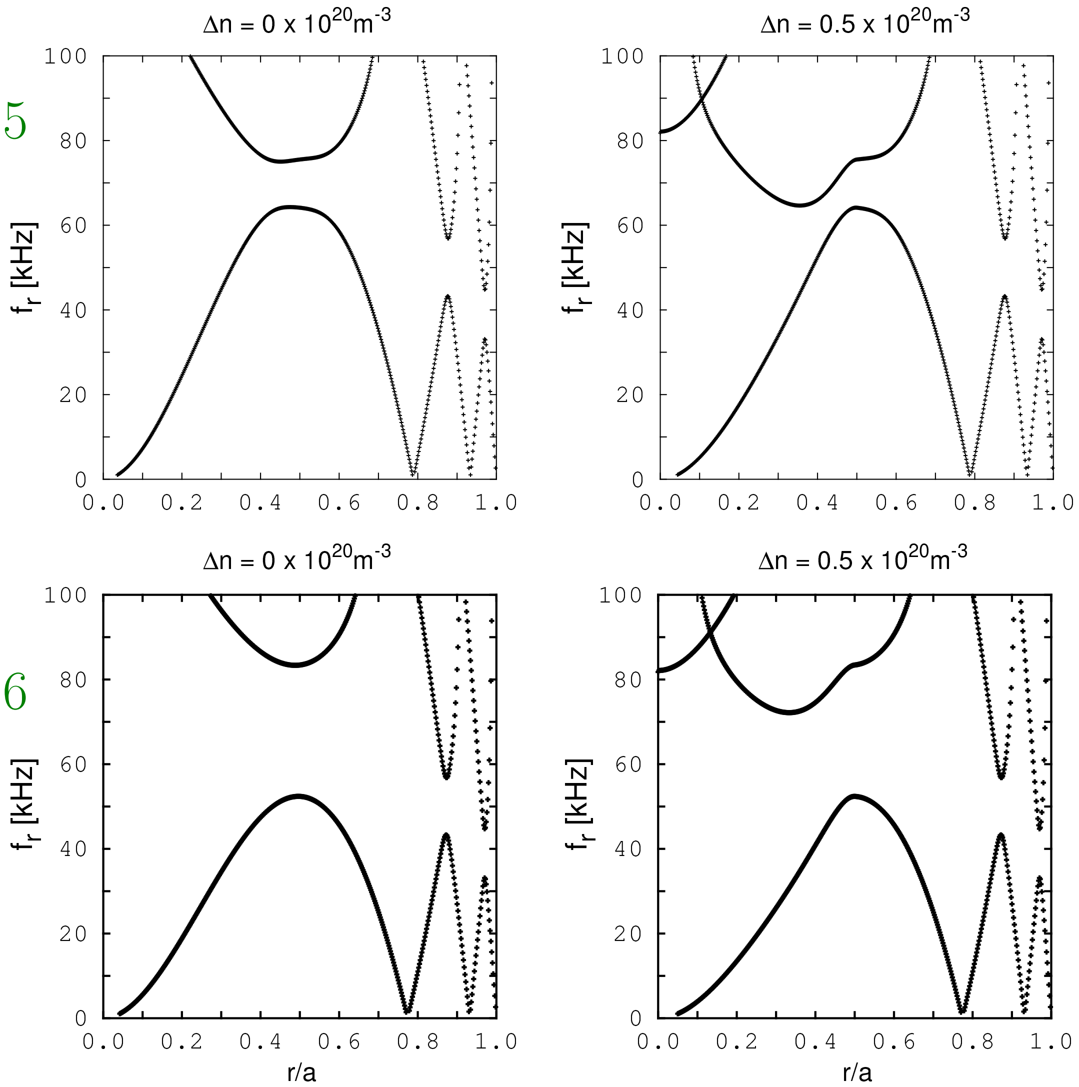

Damping Rate and Eigenfunction

Eigen frequency and damping rate

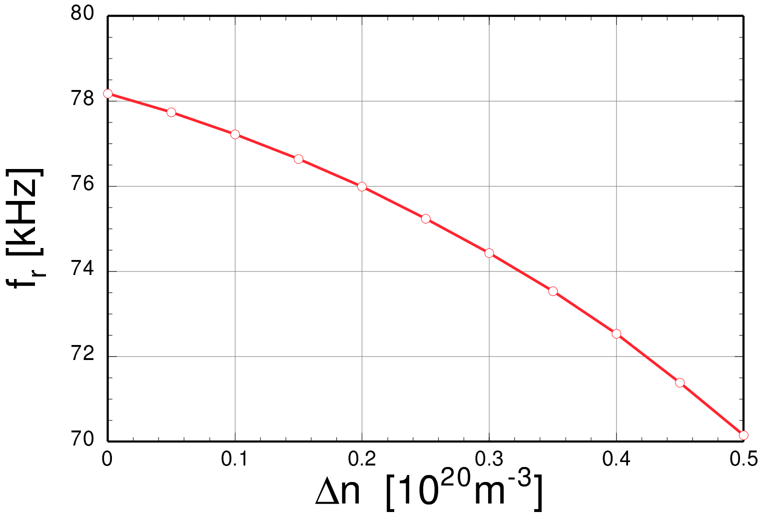

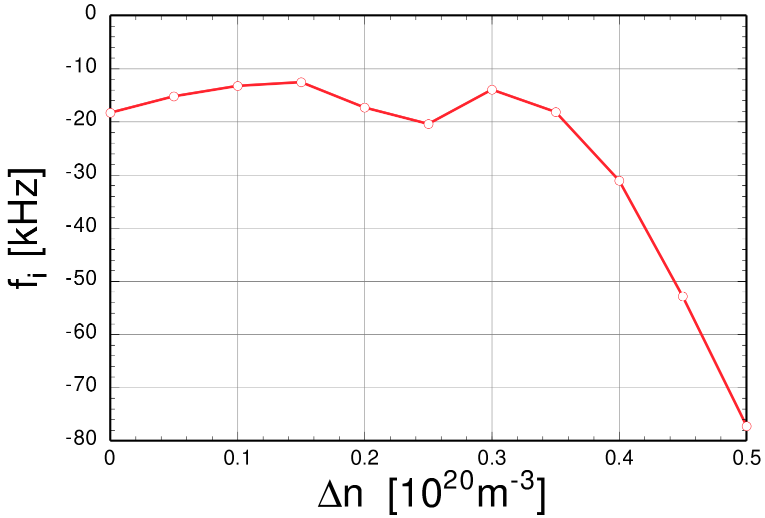

Eigenfunction

$\Delta n = 0.0$

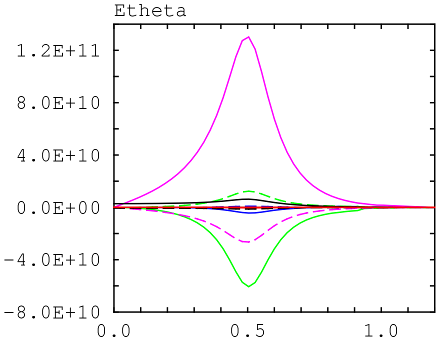

$\Delta n = 0.2$

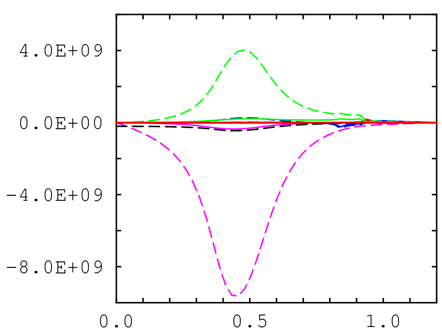

$\Delta n = 0.4$

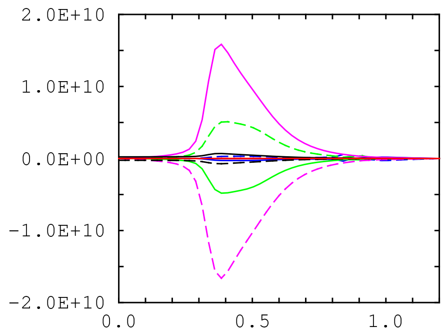

$\Delta n = 0.5$

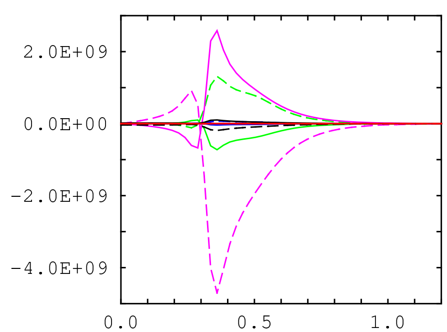

Summary

- **We studied ICRF waves in a toroidal helical plasma and Alfvén eigenmodes in tokamak plasmas using the 3D full wave code, TASK/WM.**

- **Characteristics of ICRF heating in LHD was studies using the cold plasma model. Dependence on the minority ion ratio agrees with experimental observation.**

- **The toroidal rotation changes the TAE frequency mainly through the change of gap position and q value.**

- **Destabilization by co-rotation agrees with experimental observation in JT-60U, though the stability is sensitive to the Alfvén resonance near the plasma surface.**

- **The mode structure of the EPM/RTAE below the gap frequency was studied. Two types of modes can be destabilized by the energetic ions; strongly damped TAE mode and weakly damped shear Alfvén mode.**

- **Reversed magnetic configuration supports GAE with single dominant poloidal mode number. The eigen frequency is close to the lower bound of the frequency gap and increases quickly with the decrease of q_{min}. The density jump at ITB usually stabilizes TAEs.**

- **Future work**
  - **Kinetic analysis of ICRF heating in LHD**
  - **Systematic analysis of EPM/RTAE destabilized by energetic ions**
  - **Kinetic Analysis of low-frequency modes including the effect of particle orbit**